



OPTIMIZATION OF DG UNIT SIZE AND PLACEMENT IN RADIAL DISTRIBUTION NETWORKS USING AN SLFO-BPSO HYBRID APPROACH

Engr. Junaid Zaheer, Dr. Muhammad Ifthikhar Khan

Department of Electrical Engineering

University of Engineering & Technology Peshawar, Pakistan

Fawwad Hassan Jaskani

Department of Computer Systems Engineering,

Islamia University of Bahawalpur, Pakistan

Abstract—The addition of distributed generation (DG) to an integrated delivery system has significantly increased the system's performance and efficiency. Researchers have proposed a number of alternative approaches to delivery system planning with DG insertion. In this article, a multi-objective approach is introduced to optimise both the delivery system operator's and the DG owner's reciprocal benefits. The reason behind this multi-objective approach is the inconsistent relationship between DG MVA rating reduction and device power losses reduction. To minimize system active power loss while also reducing DG size, the best compromise size of DGs in MVA, their operating power factors, and positions are obtained. The radial delivery system of IEEE-69 buses is called test system. Using the multi-objective Shuffle Frog Leap Algorithm (SFLA) for optimization, the Pareto-front of non-dominated solutions can be found. The SFLA algorithm's efficiency is equivalent to that of the Binary PSO (BPSO) algorithm. The result of the best compromised solution of DGs placement in the delivery system is measured using various system operating indices such as active power loss, reactive power loss, and voltage variance.

Keywords—MOO, GA, ML, hybrid Model, optimization techniques

I. INTRODUCTION

Recent advancement in Power Systems in the form of non-centralized generation units known as Distributed Generation (DG) Units directly tied up to the local network of DISCO's (Distribution Companies) have been proven to have a substantial impact on the quality of power flow, continuity of power flow, stability and voltage profile for the consumers of Supply Companies [1]. One of the major challenges for the Design Engineers of Power Systems is the optimal placement

of DG's. Researchers have already devised various methods to find the optimal placement location of DG units in the vicinity of distributed networks, like the Two-degree Gradient method, Lagrange Method, Sensitivity Analysis method etc. are all been used for the optimal placement of DG units [1]–[4]. These challenges for identification of best location for DGs in the distribution networks attracted substantial research efforts so that finding the optimal DG Placements for the given size of DG units & finding the Optimal sizes of the DG's on the predefined placement location are very important & significant in the scope [5]–[8].

Although DG's technology has a significant attraction as it can bring improvement in efficiency of the distribution networks [3] but the studies show that if there is inaccurate placement or sizes of DG's in the network it may happen that the power flow in the feeders may get reversed resulting in low voltage profile and high power losses in the distribution networks [4]. Although various attempts have been made on optimization of DG placement & its size so that the efficiency & reliability of the distribution systems are being improved but still there is a need for a comprehensive study so that optimal placement, optimal sizing & Optimal allocation of DG's may be defined for various scenarios in power system [9], [10].

Over the recent last years, the power industry & researchers have the main concerns for finding new strategies of how to schedule the distribution system in terms of enhancement of the efficiency. In order to overcome this problem two strategies were attracted towards the researchers; one is the expansion of network and the other is allocation of DG's in the existing distribution network [15] [16]. Knowing the fact that the high costs and environmental problems will limit the expansion in distribution networks, DG Units allocation strategy is the most feasible solution [17], [18]. In order to improve the system efficiency after the integration of DG's many important DG Parameters will need to be chosen appropriately. In this regard, various kind of approaches were



published in research for optimal DG Placement, sizing and optimal number of DG's allocation [1], [11]–[13].

In [22] [23] several sensitivity indices based approaches were presented to optimally allocate DG's on the basis of reduction in power loss of distribution system. In [24], the voltage stability index based approach was used for DG placement and allocation with objective of voltage magnitude enhancement. This was nonlinear programming technique were proposed for optimal DG placement & sizing with objective of reducing the number of DG's and increasing VSM (Voltage Stability Margin). Similarly, various kind of AI (Artificial Intelligence) [25] techniques were suggested for DG sitting & sizing. Although continuous attempts have been made to improve the reliability and efficiency of the distribution networks, however there is still a great need for a comprehensive study so that DG's may be placed, sized and allocated in an optimal way [14]-[19]

In the above-context, the proposed research work is used:

- To implement a Multi-objective approach for optimized placement& sizing of DG so that to gain improvement in the Voltage-profile & stability along with the reduction in the power losses of the distribution network.
- To optimally locate and size the DG in distribution system along with the optimal number of DG's allocation so that voltage profile of the distribution system is enhanced, system power losses due to DG integration are further reduced.
- Voltage stability of the distribution system is increased with investigation for stable busses in system for DG placement and sizing.
- To increase the efficiency of distribution networks after the non-centralized DG's integration in the system.

Figure (1) shows the proposed case study architecture in which BPSO algorithm is set to define the optimal size and site of DG's in distribution networks. In this flow map, the fitness value of the particles in the swarm show the optimal placement and size of DG in the distribution network which further help to enhance the voltage profile and minimize the active power losses of the system.

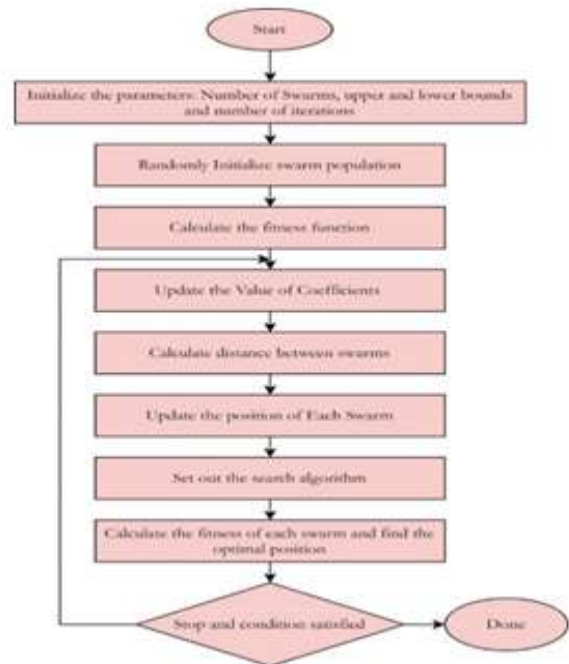


Figure 1: Proposed Architecture

The main aims & objectives of this article are:

- Multi-objective approach will be proposed in which Sensitivity Indices technique & Quadratic Curve Fitting technique will be used for optimal placement & sizing of a single DG in the distributed networks.

However, for Multiple DG's placement & sizing, the proposed work will use the Power Loss Reduction Index & the Loss Improvement Index

- The proposed approach will be applied to the IEEE 33-bus radial distribution network and power system modeling and simulation results will be carried out via MATLAB \PSAT (Power System Analysis Toolbox).
- Finally the simulation results will be analyzed for correctness & effectiveness of the proposed approach in terms of Voltage Profile Improvement (VPI), power loss reduction and maximum loading of the power system.

In the above-context of the proposed method, a multi-objective approach will be used for the optimal DG placement and it optimal sizing , basically in its theme of enhancing the voltage magnitude and minimization of power losses in distribution network of a supply company as follows;

- 1) Voltage Profile Improvement (VPI) approach of DG Placement.
- 2) Voltage Stability Enhancement (L-Index) approach of DG Placement.
- 3) Power Loss Reduction (LSF) approach of DG Placement.



II. LITERATURE REVIEW

In this section we will discuss the previous studies related to the improvement of quality of experience in a radial distribution network. Distributed generators (DG), based on renewable energy technologies are becoming popular as they address climate change and energy security issues to some extent. Renewable energy based DGs do not contribute to GHG emission and also diversity of sources also increases due to different renewable energy options that address energy security concerns. Apart from climate change and energy security concerns, there are other driving forces for increasing penetration of DG in distribution system. There are several advantages of DG in three categories: environmental, economic and technical. First, the example advantages of environmental are low emission and low noise. Second, the example advantages of Economic are saving transmission and distribution line investment cost, reducing wholesale electricity price.

Last, the example advantages of technical category are decreasing system active power losses, removal of some power quality problems, improving voltage profile, improving voltage stability index, continuity and reliability. The share of DGs in power systems has been fast increasing in the last few years. Studies have indicated that inappropriate selection of the location and size of DG may lead to greater system losses than losses without DG. Utilities already facing the problem of high power loss and poor voltage profiles cannot tolerate any increase in losses. By optimum allocation, utilities take advantage of a reduction in system losses, improved voltage regulation and an improvement in the reliability of supply [1], [20], [21]. It will also relieve the capacity of transmission and distribution systems and hence defer new investments which have a long lead-time. Distributed generation systems require high initial investment cost, which is recovered over the period through the revenues and saving, but they will incur operation and maintenance cost. In addition, the modular and small size of the DG will facilitate the planner to install it in a shorter time frame compared to the conventional solution. It would be more beneficial to install in a more decentralized environment where there is a larger uncertainty in demand and supply. However, given the choices, they need to be placed in appropriate locations with suitable sizes. Therefore, analysis tools are needed to be developed to examine locations and the sizing of such DG installations [22]–[26].

In order to reduce the overall cost of the operating system, the noise production, consumption of fuels and to mitigate the environmental affects the trend in the aircrafts is shifting from hydraulic, mechanical and pneumatic to electrical as the energy acquired from electrical source is more consistent and play a major role in green transportation[27],[28]. The electrical energy is used for most of the propulsion system, flight control operations, heating and cooling, wing de-icing and in major other auxiliary systems[29]. Recent aircrafts like

Airbus A380 and Boeing 787 has more electrical technologies installed in it and more to be installed in the near future[30].

The starter generator (S/G) system is the most important part of electrical aircrafts to provide the thrust. Previously, a variable speed variable frequency system along with the wound field synchronous starter generator system was used. But as it is AC system so to attain the parallel connection between different sources is somewhat difficult due to the different frequency and load angles. Also the excitation process is difficult so permanent magnet synchronous machines are used recently. PMSMs has high power density, high speed operation, high voltage and offer reduce weight[29],[28], [31].

A number of electrical control methods for the future Radial Systems have been suggested. The distribution of loads between multiple generation or storage elements remains complex and has been resolved by Gao et al. [32], [33]. The growing popularity of Model Predictive Control (MPC) has led to the creation of Dunham et al[34] rate-based MPC, which has mitigated the problem of adding pulse loads by predicting potential load modifications. Pulsed loading leads to Herrera et al. MPC technique for balancing generation sources and retaining bus voltage. Market-based control were promoted in non-aviation application, including more electrical ships, by Zhang et al. [9], MPC by Vu et al and by intelligent agents by Huang et al.[32], [33].

Here we all are designing the basic modeling and control architecture, which is versatile and connected to a comprehensive aircraft with examples comparable to those in [32], [35]. We also research the results of the HSSPFC-controlled lower production injection points.

A new pattern in aircraft weapons as well as protection systems is to utilize focused energy systems that heap high yield transports. These gadgets likewise have a high requests for cooling, that additionally conveys electricity by coolant siphoning or stressing loads. To befuddle the gadget more, the aircraft's thermal warmth signal should be limited to forestall detection.

Any warmth age should hence be situated inside the skin and the interior subsystems of aircraft. The utilization of the installed fuel saves as a thermal mass is a typical strategy for cooling such pulsed power systems. The fuel can be heated until 162.8 C, and the cooling loop should end. It studies the relation between thermal and electrical systems and examines the optimum energy operation of the cooling systems. We research the operative effects of reducing exercise destruction within pulsed loads of the cooling system. The automotive industry is seeing significant increase in all-electric and hybrid drivetrains. On unmanned aerial vehicles (UAVs), generally aviation (GA) and industrial aviators, related principles were researched and implemented [34], [36]. Hybrid electric propulsion systems (HEP) enable increased fuel usage for aircraft, decreased emissions, decreased take-off and landed noise, increased bandwidth efficiency and improved operating capability. Many latest HEP-powered UAV and GA aircraft



have shown almost 50% and 40% fuel economy, in high-faith simulations, however, when the same non-HEP airframe is used for the identical task.

Multi-Objective Optimization

For best and optimal solution or value, an optimization process can be used. Optimization problems consist of one or multi-objective or looking for minimum or maximum value. MOO is referred to as; the problems which have more than a single objective. This kind of problem can be seen in daily life like in engineering, mathematics, economics, social studies, agriculture, automotive, aviation and several others. In various everyday problems, the objectives that are under consideration mess with one another. And the optimizing a specific solution for a particular objective can result in undesirable results to the other objectives. A sensible and realistic solution to a multi-objective problem is to examine all solutions, every solution which fulfills the objectives at a suitable level without being conquered or dominated by any additional solution. So, according to our work, two algorithms are developed GA and NSGA-II especially for the problems with several objectives. GA and NSGA-II are meta-heuristic that are most suitable for different types of problems discussed in the next portion. On the other hand, traditional GA and NSGA-II are modified to provide multi-objective problems by presenting procedures to support solution variety and the use of particular fitness functions [37]–[43].

By imitating the biological behaviour of certain animals, swarm-based nature meta-heuristic algorithms are used to solve optimization problems. The whale optimization algorithm was proposed by Mirjalili and Lewis to simulate the hunting behaviour of humpback whales, and it works in two ways: first, by chasing the prey with a random or the best search agent, and second, by simulating the bubble net hunting strategy. Humpback whales prefer to hunt a school of small fish near the surface of the water. As a result, they swim around the target inside a thin circle to create a winding-shaped path, forming distinct blebs along a circle or a '9' shaped path altogether

III. PROPOSED ALGORITHM

The radial distribution method eliminates real power losses by dynamically positioning DGs to raise voltage profiles and lowers network running costs, which are subject to a number of operational restrictions. Mathematically, the problem's objective functions are written down. This thesis utilizes an innovative method focused on BPSO-SLFA to resolve concerns such as optimum DG sizing and positioning in the delivery system.

3.1. Major contribution of this research work

The algorithm is first used to solve the optimal DG location dilemma, which determines the best location for connecting DGs and determining their values for reconfiguring in a

momentary direction. To determine the effect and efficiency of the proposed method, the simulated results are contrasted to those of other proposed techniques. Figure 7 illustrates a flow map illustrating the proposed BPSO-SLFA.

3.2. Proposed hybrid algorithm

3.2.1. Basic Particle Swarm Optimization (BPSO)

In the year 1995, James Kennedy and Eberhart hosted BPSO, a classical kind of optimization shown in figure 2. The fitness values for this Particle Swarm Optimization are derived by the trajectory movement of the (swarm) community of people (particles). The particle is defined by an n-length vector that indicates its location, as well as a vector v that updates its current position.

The velocity vector is calculated according to the following equation in below:

$$V_{k+1}^i = \omega \cdot V_k^i + C1 \cdot R1 \cdot (P_{best}^i - X_k^i) + C2 \cdot R2 \cdot (P_{global}^i - X_k^i)$$

The random functions are R1 and R2, and where the training coefficients are C1 and C2. This is the dimension of inertia weight. The following result can be defined by:

$$\omega = \omega_{max} - \{(\omega_{max} - \omega_{min}) - k_{max}\} \times k$$

$$X_{k+1}^i = X_k^i + V_{k+1}^i$$

The PSO formula remained unaffected. A logistic conversion S(Vik) is used to achieve this amendment that is written in 5

$$S(V_{k+1}^i) = \text{sig mod } e(V_{k+1}^i) = \frac{1}{1 + \exp(-V_{k+1}^i)}$$

$$\text{If rand} \propto S(V_{k+1}^i) \text{ then: } X_{k+1}^i = 1;$$

$$\text{Else: } X_{k+1}^i = 0;$$

The function S (Vik) is a restrictive sigmoid for achieving a new change and rand is a quasi-quantity selected from a constant distribution in the space of [0, 1]. However,



$$1 \propto B_i \propto B_{max}$$

$$0 \propto P_i \propto P_{max}$$

$$T_i = \{1, 2, \dots, T_f\}$$

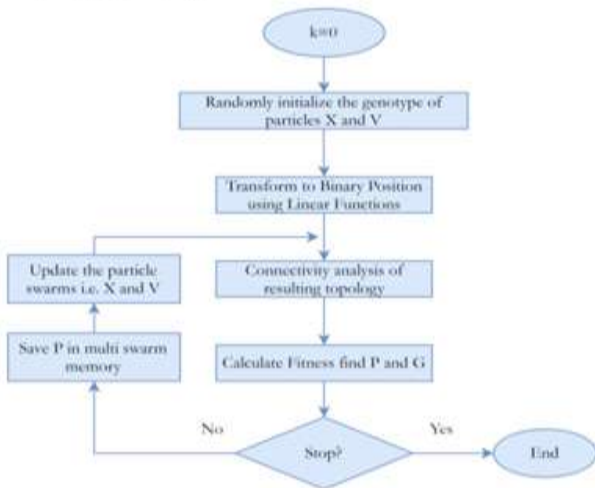


Figure 2: Basic proposed architecture of Binary Particle Swarm Optimization

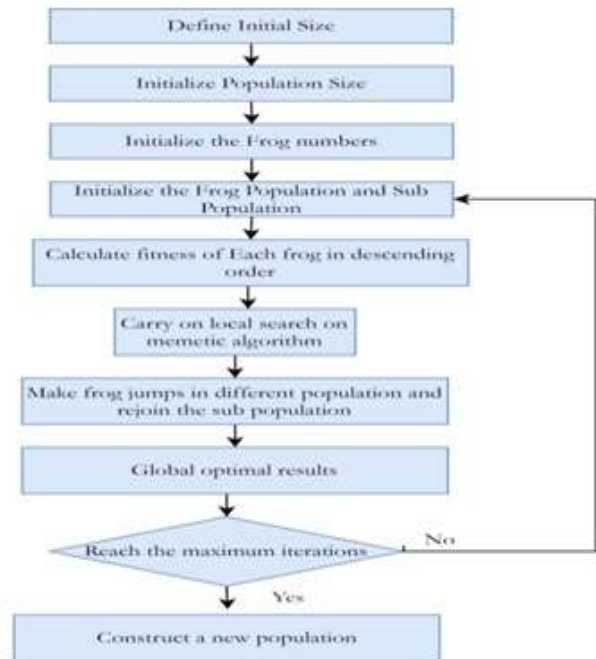


Figure 3: Shuffled Leaping Frog Algorithm

3.2.2. The Shuffled Frog-Leaping Algorithm

The SLFA algorithm, a memetic meta-heuristic for producing hybrid optimization, was created by Eusuff et al. (2017). This algorithm is a metaheuristic optimization strategy that simulates the memetic development of a community of frogs when attempting to locate the best place with the most food. In heuristic quests, memetic algorithms are updated based on population approaches to optimization problems. Dawkins invented the phrase "meme" to define the phenomena (1976). The Selfish Gene is a novel about a gene that allows humans to be selfish. n.d., Oxford University Press). The meme is believed to be the unit of human evolution. The SLFA includes a population-based solution known as memeplexes, which are separated into a subset, and the principle progresses in a similar manner to biological evolution. Specific frogs inside each memeplex have a knowledge of the other frogs, which allows them to disperse the template. Over time loops, the SLFA algorithm develops in the process of memestic growth. Any network parameters must be met in order to achieve this goal. Objective Function=Min (TLP), where $TLP = \sum_{i=1}^n I_i^2 R_i$ for the radial distribution system, R_i is the total lack of real control. The voltage is limited by the $|v_{min}| \leq |v_i| \leq |v_{max}|$ constraint. I_i is the overall fluid current over the i th branch, which reflects the DG's location and size characteristics. Branch resistance is denoted by R_i , and the number of divisions in the scheme is denoted by n . V_{min} and V_{max} are the i th bus voltages' lower and higher limits, respectively. Below figure (3) shows the SFLA flow chart.

The SFLO estimate joins the advantages of BPSO calculations based on inherited and social behavior. For S-dimensional variables problems, a frog i is defined below. (15) $X_i = (x_{i1}, x_{i2}, \dots, x_{is})$

Afterward, the frogs are sorted in relation to their fitness in a downward order. The entire population is broken into memeplexes, each with n frogs ($p = m \times n$). The best and worst-fit frogs are identified as x_g . Then, a method similar to BPSO is implemented in each step to boost only the worst-fit frog in every complete cycle. Consequently, the frog's location having the worst suitability is modified as follows: The frog position deviations are defined as:

$$D_i = rand() \times (x_b - x_w)$$

$$\text{New position } X_w = \text{current position } (X_w + D_i)$$

$$D_i = rand() \times (x_b - x_w)$$

$$\text{New position } X_w = \text{current position } (X_w + D_i)$$

The inequality that satisfies the fitness of the position is defined by $D_{min} \geq D_i \geq D_{max}$ where, $rand()$ is defined as a



random number between 0 and 1 and D_{max} is the maximum permissible change in a frog's position.

If this approach increases the performance, it substitutes the worst frog; otherwise, it would be reused, now with the better global frog in mind (replaces). If no improvements are possible, a new solution will be created at random to replace the frog. To reduce losses and improve voltage profile, SFL algorithm is used to optimize the position and power of the DG. The below is a description of the steps in order: Figure (4) displays a flow map representing the estimated BPSO-SLFA.

3.3. Proposed Methodology of BPSO-SLFA

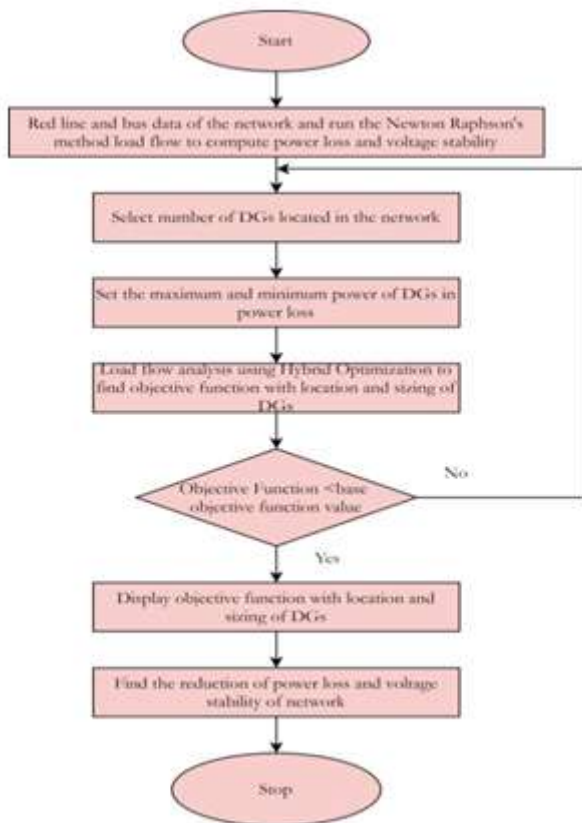


Figure 4: A proposed flowchart for the algorithm

The flowchart for deciding the direction and scale of the DG to be detected is shown in Figure (4). The measures below detail the strategies for deciding the optimum size and location of DGs using the suggested hybrid optimization algorithm.

Phase 1: Data from the input line and data from the bus are the first two stages.

Phase 2: Settle about the amount of DG units to use in the network for the best positioning.

Phase 3: For the DGs, set the voltage limits with actual and reactive control limits, and the power factor for the DGs is set according to the reactive power compensation required.

Phase 4: Conduct a load flow study to assess the overall active power failure while preserving voltage stabilization.

Phase 5: Organize the algorithm parameters, such as frequency duration, pulse rate, loudness, and iterations.

Phase 6: Iteration is accomplished using a hybrid optimization algorithm with an objective function that is both powerful and reliable.

Phase 7: In each iteration, the location and size of the DGs are chosen at random while the frequency, velocity, and position are modified.

IV. EXPERIMENTAL RESULTS

4.1. Overview

Different scenarios are considered for the location of several DGs in a 69-bus radial distribution system and an 85-bus radial distribution system. To minimize active power loss and the size of DGs in MVA, the BPSO and SFLO algorithms are employed. The Pareto-fronts of non-dominated solutions are calculated for a variety of scenarios. The locations, weights, and operating power variables of the DGs were calculated for non-dominated solutions. For each Pareto-front three points, the letters A, B, and C are highlighted. The solution with the lowest value of objective-1 (active power loss) and the highest value of objective-2 is represented by the point A. (DG size in MVA). The best compromise solution is shown by the letter B. By point C, the maximum value of objective-1 and the minimum value of objective-2 are represented. The solution is determined by the test system's topology and loading state. For the presented problem, the efficiency of the SFLO (Shuffle Frog Leap Algorithm) and BPSO (Binary particle swarm optimization) algorithms was contrasted using a 69-bus radial distribution method as a test case.

4.2. IEEE 69 Bus radial distribution system

For case studies, the IEEE 69-bus radial distribution method (shown in Figure 5) is used. Bus1 represents the sub-station. This system's base MVA and base voltage are 100MVA and 12.66 kV, respectively. The active power load on this system is 3.8 MW, and the reactive power load is 2.69 MVar. The system's active power loss is 0.225 MW and its reactive power loss is 0.1022MVar in the worst-case scenario (no DG). The minimum voltage is at bus 65 in the base case (0.9092 p.u.).

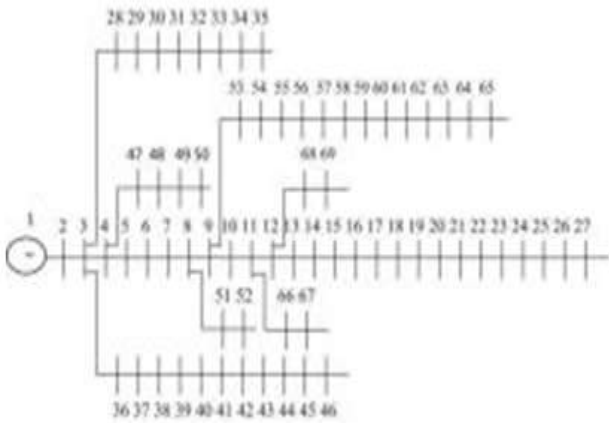


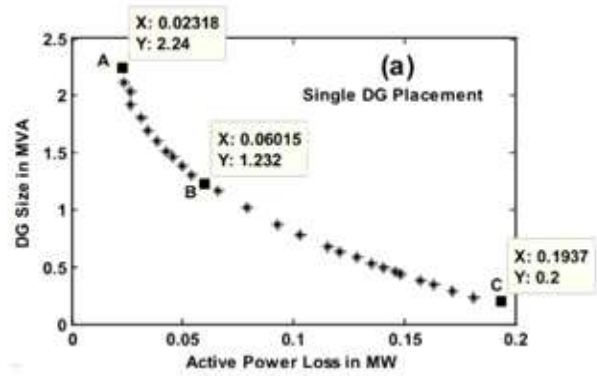
Figure 5: IEEE-69 Buses Radial Distribution Network

4.1.1 Case A:

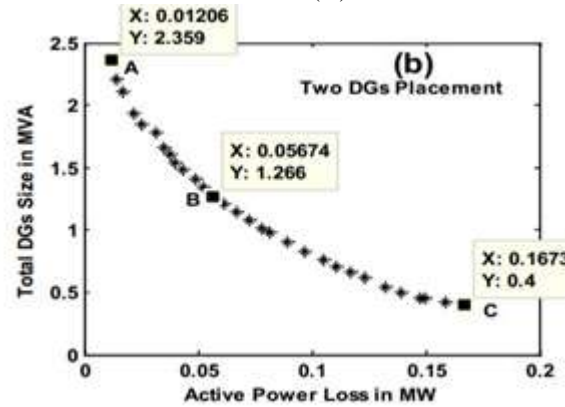
The maximum active power injection capability of the DG is 50% of the active power load of the machine. Complete active power injection by DGs is presumed to range between 0.2 and 1.91 MW in this study. The maximum active power injection capability of the DGs is limited to 50% of the test system's overall active power load. The difference in power factors ranges from 0.8 to 1. Figure 6 show the Pareto-fronts of non-dominated options, as well as empirical outcomes for various scenarios.

4.1.1.1 Scenario 1: Single DG placement

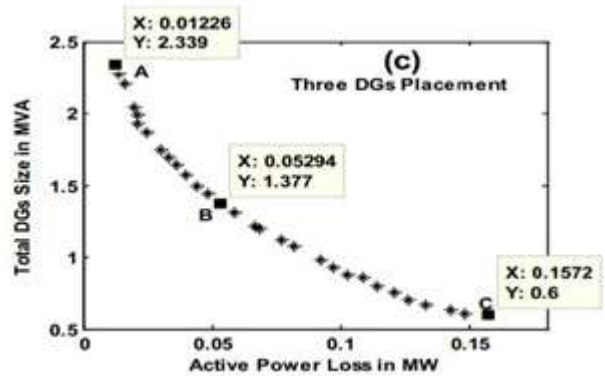
When using the smallest DG scale available in MVA, the use of a single DG has been considered to minimize system active power loss. With non-dominated alternatives, it was possible to find the Pareto-front. The DG with a scale of 2.24 MVA at bus 61 achieves the greatest reduction in active power loss, as seen in Fig. below. The DG injects active power of 1.8148 MW and reactive power of 1.3139 MVar, respectively. The active power loss is reduced to 0.0232 MW, while the reactive power loss is reduced to 0.0144 MVar. From 9.08 percent to 2.76 percent, the VDI has been reduced. The minimum unit bus voltage at bus 27 is observed to be 0.9724 p.u. The Paretofront best corrupted solution (point B) is achieved using a DG scale of 1.232 MVA at bus 61. The DG injects active power of 0.9858 MW and reactive power of 0.7393 MVar, respectively. The active and reactive power losses in this system are both limited to 0.060 MW and 0.0316 MVar, respectively. The VDI has dropped to just 4.09 percent. The minimum bus voltage at bus 65 is found to be 0.9591 p.u.



Point (A)



Point (B)



Point (C)

Figure 6: Pareto-front of non-dominated solutions for single, two and three DGs placement in IEEE 69-bus system

4.1.1.2 Scenario 2: Two DGs placement

The combined potential of overall active power injection by DGs is limited to 1.91 MW when two DGs are used. The highest reduction in active power loss is achieved with total DGs size of 2.36 MVA, as seen in Fig. 6 from the Pareto-front of non-dominated solutions (Point A). The DGs pump 1.9 MW of active power and 1.3959 MVar of reactive power, respectively, into the grid. Active and reactive power losses



have been limited to 0.012 MW and 0.010 MVA_r, respectively. The VDI has been lowered to 1.32%. At bus 17, the minimum device bus voltage is found to be 0.98684 p.u. With a total DGs size of 1.26 MVA, the Paretofront strongest corrupted solution (point B) is obtained. The DGs inject 1.022 MW of active and reactive power, respectively, and 0.7463 MVA_r of reactive power. The active and reactive power losses are both limited to 0.057 MW and 0.030 MVA_r, respectively, in this case. The VDI is now just 3.73 percent. At bus 65, the minimum bus voltage is found to be 0.9627p.u

4.1.1.3 Case 3: Three DGs placement

The maximum potential of overall active power injection by DGs is limited to 1.91 MW when three DGs are installed. The highest reduction in active power loss is achieved with total DGs size of 2.33 MVA, as seen in Fig. 9 from the Pareto-front of non-dominated solutions (Point A). The DG's combined active and reactive power injections are 1.876 MW and 1.383 MVA_r, respectively. The active and reactive power losses are cut in half, to 0.011 MW and 0.009 MVA_r, respectively. The VDI has been lowered to 1.22%. At bus 16, the minimum device bus voltage is found to be 0.98784p.u. With a total DGs size of 1.38 MVA, the Paretofront strongest corrupted solution (point B) is obtained. The DGs pump 1.154 MW of active power and 0.7128 MVA_r of reactive power, respectively, into the grid. The active and reactive power losses are also limited to 0.053 MW and 0.029 MVA_r, respectively, in this case. The VDI has been lowered to 3.85%. At bus 65, the minimum bus voltage is found to be 0.9615 p.u.

4.1.2 Case B:

The total active power load of the test device is represented by the DG maximum active power injection capability. The average active power injection by DGs is assumed to be between 0.2 and 3.8 MW in this study. The difference in power factors ranges from 0.8 to 1. Figure 7 show the Pareto-fronts of non-dominated options, as well as empirical outcomes for various scenarios of case B.

4.1.2.1 Scenario 1: Single DG placement

For single DG positioning, the capability of active power injection by DG is presumed up to 3.8 MW. The maximum reduction of active power loss is obtained with DG size of 2.24 MVA at bus 61 as seen in Fig. 7a (Point A) (Point A). The cumulative active power and reactive power injections by the DG are 1.8148 MW and 1.3611 MVA_r respectively. The active power loss reactive power loss was reduced to 0.0232 MW and 0.0144 MVA_r respectively. The VDI is reduced to 2.76 percent. The minimum circuit bus voltage is observed to be 0.9724 p.u. at bus 27. The optimal compromised solution (point B) of the Paretofront is obtained with total DGs size of 1.23 MVA at bus 61.

The active power and reactive power injections by the DG are 0.9858 MW and 0.7393 MVA_r respectively. Here, the active power loss and reactive power loss are limited to 0.060 MW

and 0.032 MVA_r respectively. The VDI is reduced to 3.85 percent. The minimum bus voltage is observed to be 0.9591 p.u. at bus 65. Comparing single DG positioning study for 69-bus radial delivery system with two separate active power injection volume maximum limits, it is concluded that the maximum reduction of active power loss is obtained with DG size of 2.24 MVA at bus 61.

4.1.2.2 Scenario 2: Two DGs placement

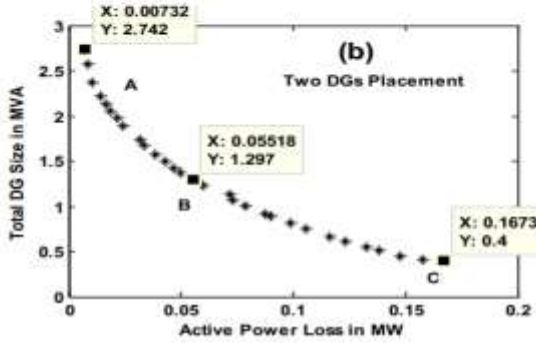
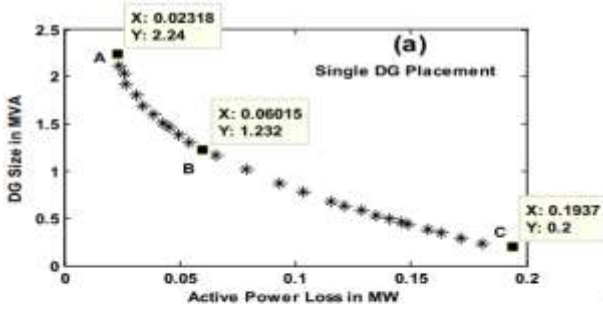
As seen in Fig. 7b, with two DGs in position, the optimal reduction in active power loss is achieved with a total DGs scale of 2.74 MVA (Point A). The DG injects a total of 2.467 MW of active power and 1.593 MVA_r of reactive power, respectively. The active and reactive power losses have both been limited to 0.0073 MW and 0.0081 MVA_r, respectively. The VDI has been lowered to 0.58%. At bus 69, the minimum system bus voltage is found to be 0.9942 p.u. With a total DGs size of 1.3 MVA, the Paretofront's strongest corrupted solution (point B) is obtained. The DGs pump 1.038 MW and 0.779 MVA_r of active power and reactive power, respectively. The active and reactive power losses are both limited to 0.055 MW and 0.029 MVA_r, respectively, in this case. The VDI is now just 3.79 percent. At bus 65, the minimum bus voltage is found to be 0.9621p.u.

4.1.2.3 Scenario 3: Three DGs placement

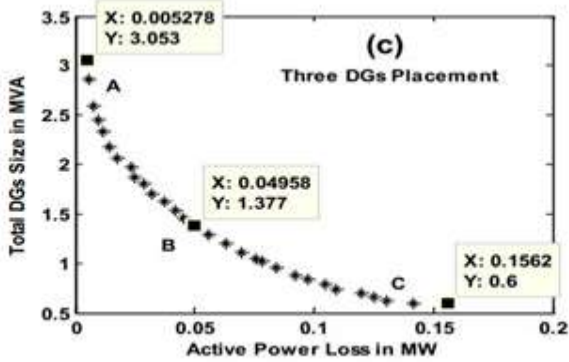
As seen in Fig. 7c (Point A) with three DGs positioning, the maximum reduction in active power loss is achieved with a total DGs size of 3.5 MVA. The DG injects a total of 2.47 MW of active power and 1.795 MVA_r of reactive power, respectively. The active power loss is now 0.0053 MW, and the reactive power loss is now 0.0072 MVA_r. The VDI is now just 0.57 percent. At bus 50, the minimum device bus voltage is found to be 0.9943 p.u. With a total DGs size of 1.38 MVA, the Paretofront's strongest corrupted solution (point B) is obtained. The DG injects 1.156 MW of active power and 0.797 MVA_r of reactive power, respectively. The active and reactive power losses are limited to 0.0496 MW and 0.0269 MVA_r, respectively, in this case. The VDI has been lowered to 3.34%. At bus 27, the minimum bus voltage is found to be 0.966 p.u. Figures 9 and 10 depict the various Pareto-fronts of non-dominated options for various scenarios. The x axis magnitude of the lowest point of each Pareto-front is non-zero since the minimum DG size in MW is set to 0.2 MW. In the given search space, the Paretofront provides a well-spread of solutions.



Point A



Point B



Part (C)

Figure 7: Pareto-front of non-dominated solutions for single, two and three DGs placement in IEEE 69-bus system of case B

4.2. Comparison of Multi Objective Optimization Techniques

For case B cases, the efficiency of the SFLA algorithm is compared to the performance of the BPSO algorithm. In comparison to BPSO, the Pareto-front of SFLA provides a well-spread of non-dominated solutions in the specified search space, as seen in Figures 8, 9 and 10. In all scenarios, the best possible compromise options are found.

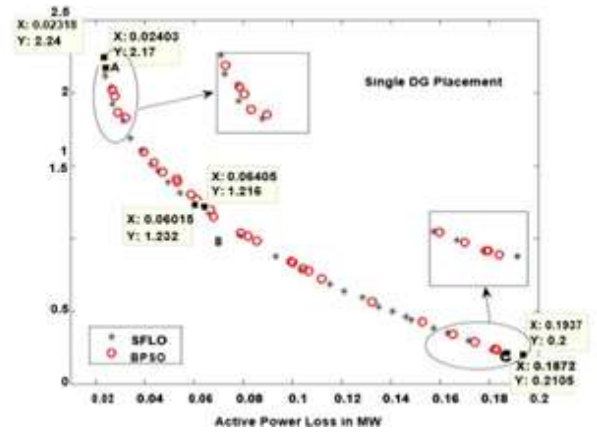


Figure 8: Comparison of Pareto-fronts of SFLO algorithm and BPSO algorithm for one DGs placement

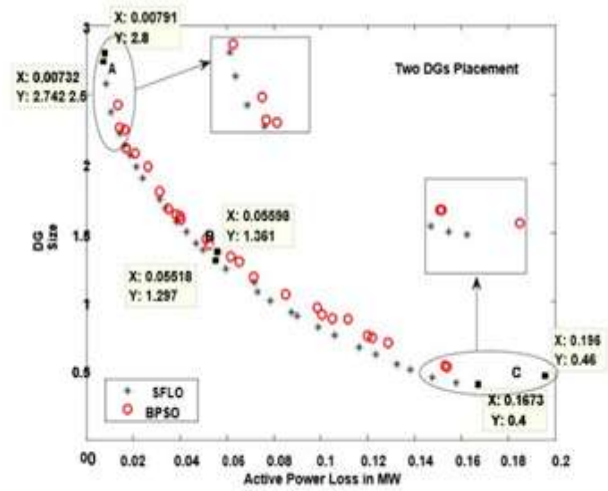


Figure 9: Comparison of Pareto-fronts of SFLO algorithm and BPSO algorithm for two DGs placement

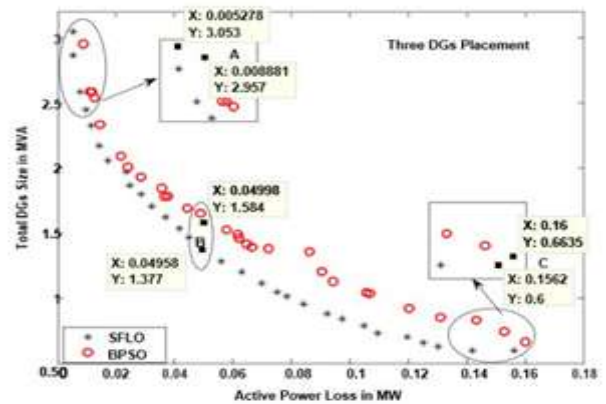


Figure 10: Comparison of Pareto-fronts of SFLO algorithm and BPSO algorithm for three DGs placement



For the better corrupted solutions, the device value indices are determined. It has been discovered that the findings obtained with SFLA are superior to those obtained with BPSO. The effectiveness of every optimization algorithm is determined by the problem's existence. SFLA is found to do better than BPSO in the presented work. The bus voltage profile is improved by the active and reactive power injection by DGs in the delivery system. Figure 11 depicts the increased bus voltage profile in case B for various scenarios. The bus 61 has a load of 1200 kW in a 69-bus radial delivery scheme, and bus 27 is the primary feeder's end bus (Fig. 11). As a result, the increase in voltage at these buses is highlighted in this voltage profile graph. As seen in Fig. 11a, the voltage of buses 65 and 27 has been increased to 0.9677 and 0.9666 p.u. for the best compromised solution of three DGs positioning with a total DGs scale of 1.38 MVA. The voltage of bus 65 is increased to 0.999 with a total DG size of 3.05 MVA, as seen in Figure 11b.

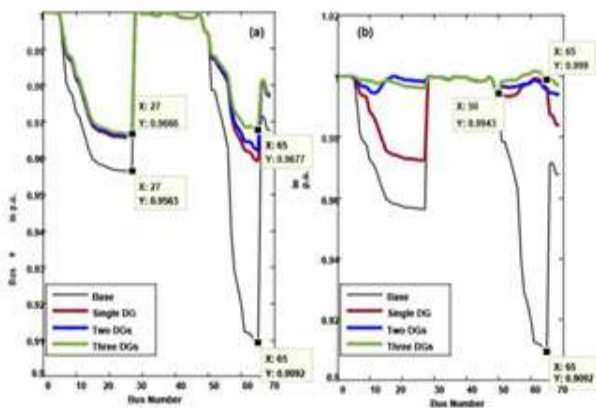


Figure: 11 Voltage profile comparison of 85-buses radial distribution system, a for compromised solution, b for solution with minimum active power loss

The set of non-dominated approaches is represented by the Pareto-front. Any of these options is available to the delivery system operator, depending on the requirements. Similarly, the existence of outlets for physical positioning of DGs has an effect on the delivery system operator's choice of solution

V. CONCLUSION

The suggested plan has been beneficial to both the distribution system operator and the DG stakeholders. A wide range of single and multiple DG positioning scenarios have been investigated. The effect of DG placement on the distribution system is measured using device performance metrics such as active power loss, reactive power loss, and voltage variance. According to case studies of different scenarios of DG insertion, reactive power injection along with vigorous power injection by the DG significantly reduces power losses while

also assisting in increasing the bus voltage profile. The Pareto-front is a set of non-dominated methods with a limited number of solutions for a variety of objective functions ranging from minimum to optimum. The distribution system operator can choose from any of these options depending on the requirements.

VI. REFERENCE

- [1] UNIDO, "Industrial Prosumers of Renewable Energy, Contribution to Inclusive and Sustainable Industrial Development," United Nations Ind. Development Organ., 2015, [Online]. Available: https://www.unido.org/sites/default/files/2015-04/PROSUMERS_Energy_0.pdf.
- [2] C. Miao, K. Teng, Y. Wang, and L. Jiang, "Technoeconomic analysis on a hybrid power system for the uk household using renewable energy: A case study," *Energies*, vol. 13, no. 12, 2020, doi: 10.3390/en13123231.
- [3] IRENA, *Climate Change and Renewable Energy: National policies and the role of communities, cities and regions*, no. June. 2019.
- [4] E. Parliament, "Luxembourg action plan for renewable energy," 2003.
- [5] TEM, "Finland's national action plan for promoting energy from renewable sources pursuant to Directive 2009/28/EC," 2010, [Online]. Available: <http://ec.europa.eu/energy/en/topics/renewable-energy/national-action-plans%0D>.
- [6] S. Shinkhede, "Implementation of the Micro- Grid Concept And Balancing Massive Energy Production from Renewable Sources," vol. 3, no. 1, pp. 76–84, 2014.
- [7] R. Majumder, A. Ghosh, G. Ledwich, and F. Zare, "Enhancing the stability of an autonomous microgrid using DSTATCOM," *Int. J. Emerg. Electr. Power Syst.*, vol. 10, no. 5, pp. 564–569, 2010, doi: 10.2202/1553-779X.2227.
- [8] H. Lotfi, A. Khodaei, S. Bahramirad, and M. Bollen, "Optimal Design of Hybrid AC/DC Microgrids," *CIGRE Grid Futur. Symp.*, 2016.
- [9] C.-T. Ma and T.-H. Shr, "Power Flow Control of Renewable Energy Based Distributed Generators Using Advanced Power Converter Technologies," *J. Clean Energy Technol.*, vol. 3, no. 1, pp. 48–53, 2015, doi: 10.7763/jocet.2015.v3.167.
- [10] R. Lasseter et al., "The CERTS microgrid concept, white paper on integration of distributed energy resources," Calif. Energy Comm. Off. Power Technol. Dep. Energy, LBNL-50829, [http://certs. lbl. gov](http://certs.lbl.gov), p. 29, 2002.
- [11] Y. C. Liang, Q. Zhang, E. G. Larsson, and G. Y. Li, "Symbiotic Radio: Cognitive Backscattering Communications for Future Wireless Networks," *IEEE*



- Trans. Cogn. Commun. Netw., vol. 6, no. 4, pp. 1242–1255, 2020, doi: 10.1109/TCCN.2020.3023139.
- [12] X. Chen et al., “Artificial intelligence-empowered path selection: A survey of ant colony optimization for static and mobile sensor networks,” *IEEE Access*, vol. 8, pp. 71497–71511, 2020, doi:10.1109/ACCESS.2020.2984329.
- [13] A. Fragkiadakis, V. Angelakis, and E. Z. Tragos, “Securing cognitive wireless sensor networks: A survey,” *Int. J. Distrib. Sens. Networks*, vol. 2014, 2014, doi: 10.1155/2014/393248.
- [14] M. C. Hlophe and B. T. Maharaj, “QoS provisioning and energy saving scheme for distributed cognitive radio networks using deep learning,” *J. Commun. Networks*, vol. 22, no. 3, pp. 185–204, 2020, doi: 10.1109/JCN.2020.000013.
- [15] G. L. Santos, P. T. Endo, D. Sadok, and J. Kelner, “When 5G meets deep learning: A systematic review,” *Algorithms*, vol. 13, no. 9, pp. 1–34, 2020, doi: 10.3390/A13090208.
- [16] N. Nurelmadina et al., “A systematic review on cognitive radio in low power wide area network for industrial IoT applications,” *Sustain.*, vol. 13, no. 1, pp. 1–20, 2021, doi: 10.3390/su13010338.
- [17] B. J. Saharia, M. Manas, and S. Sen, “Comparative study on buck and buck-boost DC-DC converters for MPP tracking for photovoltaic power systems,” *Proc. - 2016 2nd Int. Conf. Comput. Intell. Commun. Technol. CICT 2016*, pp. 382–387, 2016, doi: 10.1109/CICT.2016.81.
- [18] M. Shwetha and S. Lakshmi, “DC-DC Buck Boost Converter For Renewable and Biomedical Application based Real-Time IoT,” *Int. J. Recent Technol. Eng.*, vol. 8, no. 4, pp. 328–336, 2019, doi: 10.35940/ijrte.d6841.118419.
- [19] A. Bouchakour, L. Zaghiba, M. Brahami, and A. Borni, “Study of a Photovoltaic System Using MPPT Buck-Boost Converter,” *Int. J. Mater. Mech. Manuf.*, vol. 3, no. 1, pp. 65–68, 2015, doi: 10.7763/ijmmm.2015.v3.168.
- [20] United Nations Environment Programme, International Union for Conservation of Nature and Natural Resources, and Pace University, *UNEP handbook for drafting laws on energy efficiency and renewable energy resources*. 2007.
- [21] “Renewable Energy Markets Key to financing: Communities and Households.”
- [22] S. Kamyab and M. Eftekhari, “Feature selection using multimodal optimization techniques,” *Neurocomputing*, vol. 171, pp. 586–597, Jan. 2016, doi: 10.1016/j.neucom.2015.06.068.
- [23] Z. H. Wei and B. J. Hu, “A Fair Multi-Channel Assignment Algorithm with Practical Implementation in Distributed Cognitive Radio Networks,” *IEEE Access*, vol. 6, pp. 14255–14267, 2018, doi: 10.1109/ACCESS.2018.2808479.
- [24] H. Zhang, F. Sun, and J. Qian, “An optimization based on general airport of complex condition,” *CITS 2019 - Proceeding 2019 Int. Conf. Comput. Inf. Telecommun. Syst.*, pp. 1–5, 2019, doi: 10.1109/CITS.2019.8862029.
- [25] F. Din and K. Z. Zamli, “Fuzzy adaptive teaching learning-based optimization strategy for GUI functional test cases generation,” *ACM Int. Conf. Proceeding Ser.*, pp. 92–96, 2018, doi: 10.1145/3185089.3185148.
- [26] W. Xia, G. Zheng, Y. Zhu, J. Zhang, J. Wang, and A. P. Petropulu, “A deep learning framework for optimization of MISO downlink beamforming,” *IEEE Trans. Commun.*, vol. 68, no. 3, pp. 1866–1880, 2020, doi: 10.1109/TCOMM.2019.2960361.
- [27] Y. Zhang, J. Chen, and Y. Yu, “International Journal of Electrical Power and Energy Systems Distributed power management with adaptive scheduling horizons for more electric aircraft,” *Int. J. Electr. Power Energy Syst.*, vol. 126, no. PA, p. 106581, 2021, doi: 10.1016/j.ijepes.2020.106581.
- [28] F. Liu, L. Xu, Y. Li, Y. Kang, and Z. Wu, “Permanent magnet synchronous machine starter / generators based high-voltage DC parallel electric power system for the more electric aircraft,” no. November 2017, pp. 8–9, 2018, doi: 10.1049/joe.2018.0015.
- [29] D. Miao, Y. Mollet, J. Gyselinck, and J. Shen, “DC Voltage Control of a Wide-Speed-Range Permanent-Magnet Synchronous Generator System for More Electric Aircraft Applications,” no. Nsf 51377140, 2016.
- [30] A. Braitor, A. R. Mills, V. Kadiramanathan, and G. C. Konstantopoulos, “Control of DC power distribution system of a hybrid electric aircraft with inherent overcurrent protection,” *2018 IEEE Int. Conf. Electr. Syst. Aircraft, Railw. Sh. Propuls. Road Veh. Int. Transp. Electrification Conf.*, pp. 1–6, 2018.
- [31] Paramjitsinghkanwar & R K Sharma, “Power Quality and Voltage Stability of Transmission Line Using Statcom and SSSC,” *Int. J. Electr. Electron. Eng.*, vol. 5, no. 4, pp. 1–8, 2016, [Online]. Available: http://www.iaset.us/view_archives.php?year=2016&jty p e=2&id=15&details=archives.
- [32] G. Buticchi, M. Liserre, and K. Al-Haddad, “On-Board Microgrids for the More Electric Aircraft,” *IEEE Trans. Ind. Electron.*, vol. 66, no. 7, pp. 5585–5587, 2019, doi: 10.1109/TIE.2019.2897470.
- [33] P. Zhao et al., “Intelligent Injection Molding on Sensing, Optimization, and Control,” *Adv. Polym. Technol.*, vol. 2020, pp. 1–22, 2020, doi: 10.1155/2020/7023616.
- [34] T. J. Wall and R. T. Meyer, “Hybrid electric aircraft switched model optimal control,” *J. Propuls. Power*, vol. 36, no. 4, pp. 488–497, 2020, doi: 10.2514/1.B37419.



- [35] A. Qahouq and A. Rub, "Author index," pp. 1–162, 2011, doi: 10.1109/ecce.2011.6063737.
- [36] W. ZINE, "HF signal injection and Machine Learning for the sensorless control of IPMSM-based EV drives."
- [37] A. D. HM Harb, "Adaboost ensemble with genetic algorithm postoptimization for intrusion detection," *Int J Comput Sci Issues*, vol. 8, no. 5, pp. 28–33, 2011.
- [38] I. Syarif, A. Prugel-Bennett, and G. Wills, "SVM parameter optimization using grid search and genetic algorithm to improve classification performance," *Telkomnika (Telecommunication Comput. Electron. Control.*, vol. 14, no. 4, pp. 1502–1509, 2016, doi:10.12928/TELKOMNIKA.v14i4.3956.
- [39] R. Teeket al., "Hearing impairment in Estonia: An algorithm to investigate genetic causes in pediatric patients," vol. 58, no. 2, pp. 419–428, 2013, doi: 10.2478/ams-2013-0001.
- [40] M. Mahsal Khan, A. Masood Ahmad, G. Muhammad Khan, and J. F. Miller, "Fast learning neural networks using Cartesian genetic programming," *Neurocomputing*, vol. 121, pp. 274–289, Dec. 2013, doi: 10.1016/j.neucom.2013.04.005.
- [41] D. Papamartzivanos, F.Gómez Mármol, and G. Kambourakis, "Dendron: Genetic trees driven rule induction for network intrusion detection systems," *Futur. Gener. Comput. Syst.*, vol. 79, pp. 558–574, Feb. 2018, doi: 10.1016/j.future.2017.09.056.
- [42] R. Siva Subramanyam Reddy, T. Gowri Manohar, and M. S. Kumar Reddy, "Optimal placement and sizing of unified power flow controller using heuristic techniques for electrical transmission system," *ARPJ. Eng. Appl. Sci.*, vol. 12, no. 22, pp. 6357–6363, 2017.
- [43] A. A. Elngar, "IoT-based Efficient Tamper Detection Mechanism for Healthcare Application," *Int. J. Netw. Secur.*, vol. 20, no. March, 2018, doi: 10.6633/IJNS.201805.20(3).11